

SIMPLIFIED DESCRIPTION OF THE FIELD DISTRIBUTION IN FINLINES AND RIDGE WAVEGUIDES AND ITS APPLICATION TO THE ANALYSIS OF E-PLANE DISCONTINUITIES

R. R. Mansour*, R. S. K. Tong* and R. H. MacPhie**

*COM DEV Ltd., Cambridge, Ontario, Canada, N1R 7H6

**Department of Electrical Engineering, University of Waterloo, Waterloo, Ontario, Canada, N2L 3G1

ABSTRACT

Using closed-form equations for the field distribution of the eigenmodes in ridge waveguides, this paper presents a simplified analysis for ridge waveguide E-plane discontinuities. The accuracy of the calculated results is checked by comparison with experimental results. Closed-form equations are also presented for the field distribution of the dominant hybrid mode in unilateral finlines.

Although numerous closed-form equations have been reported in the literature [6], for calculating the propagation constant in finlines, no paper has appeared for quick and easy evaluation of the field distribution. In this paper, we also present closed-form equations for the field distribution for the dominant mode in unilateral finlines. In addition, to the practical usefulness of these equations in the design of non-reciprocal finline components [7], these equations can be also used to derive a closed-form expression for the characteristic impedance.

I. INTRODUCTION

Recently, two rigorous approaches have been reported for the characterization of ridge waveguide E-plane discontinuities [1], [2]. The first one [1] uses the spectral domain technique and has the advantage of high numerical efficiency. It is however, limited only to structures with infinitely thin ridges. The second approach [2], applies the mode matching technique and requires the determination of the field distribution of the ridge waveguide eigenmodes. In this approach [2], however, the field distribution of the TE and TM modes in the ridge waveguide is obtained by following the conventional method of solving the boundary value problem first for the eigenvalue (the propagation constant), then for the associated eigenvector. Besides its complexity, the computational effort involved in this approach is extremely large.

On the other hand, approximate closed-form equations for the field distribution of the TE modes in ridge waveguides have been reported in [3]. These equations have been also used with the variational technique in [4] to analyze slot resonators. However, due to the coupling between TE and TM modes, formulation of the scattering matrix of the ridge waveguide discontinuity requires the knowledge of the field distribution of both TE and TM modes.

In this paper, we present closed-form equations for the field distribution of the TM modes in ridge waveguides. The closed-form equations for both TE and TM modes are then used with the conservation of complex power technique [5] to provide an efficient analysis of ridge waveguide E-plane discontinuities. The validity of this analysis is verified by comparing our results with published results as well as experimental results.

II. ANALYSIS OF E-PLANE RIDGE WAVEGUIDE DISCONTINUITIES

Consider the ridge waveguide discontinuity shown in Fig. 1. This discontinuity represents the basic building block in the design of many microwave and millimeter-wave components such as matching transformers and evanescent mode filters. The major complexity in formulating the scattering matrix of this discontinuity is in determining the field distribution of the eigenmodes in the ridge waveguide region. The propagation constants of the eigenmodes in ridge waveguides are related to the cutoff frequencies which can be easily calculated according to [5]. With the assumption of a single term in the ridge gap (region II) of Fig. 2, and N expansion terms in the trough region (region I), the field distribution of the TE and TM modes can be written as:

TE modes

$$\vec{E}_I = \sum_{n=0,1,2,\dots}^N A_n \left[\frac{n\pi}{b} \cos \alpha_n x \sin \frac{n\pi}{b} y \vec{a}_z - \alpha_n \sin \alpha_n x \cos \frac{n\pi}{b} y \vec{a}_y \right] e^{-j\beta z} \quad (1a)$$

$$\begin{aligned} \vec{H}_I = \sum_{n=0,1,2,\dots}^N A_n \frac{\beta}{\omega\mu} & \left[\alpha_n \sin \alpha_n x \cos \frac{n\pi}{b} y \vec{a}_z + \right. \\ & \left. \frac{n\pi}{b} \cos \alpha_n x \sin \frac{n\pi}{b} y \vec{a}_y + \right. \\ & \left. \frac{k_c^2}{j\beta} \cos \alpha_n x \cos \frac{n\pi}{b} y \vec{a}_z \right] e^{-j\beta z} \quad (1b) \end{aligned}$$

$$\vec{E}_{II} = \cos k_c \left(\frac{a}{2} - x \right) \vec{a}_y e^{-j\beta z} \quad (1c)$$

$$\vec{H}_{II} = -\frac{\beta}{\omega\mu} \left[\cos k_c \left(\frac{a}{2} - x \right) \vec{a}_x + \frac{k_c}{j\beta} \sin k_c \left(\frac{a}{2} - x \right) \vec{a}_z \right] e^{-j\beta z} \quad (1d)$$

where

$$A_n = \frac{-\Gamma_n \cos(k_c s/2)}{\alpha_n \sin(\alpha_n l) (n\pi)} \left[\sin \frac{n\pi}{b} (h+d) - \sin \frac{n\pi}{b} h \right]$$

$\Gamma_n = 1$ for $n=0$, and $\Gamma_n = 2$, for $n=1,2,3\dots$

TM modes

$$\vec{E}_I = \sum_{n=1,2,3\dots}^N B_n \left[\alpha_n \cos \alpha_n x \sin \frac{n\pi}{b} y \vec{a}_x + \frac{n\pi}{b} \sin \alpha_n x \cos \frac{n\pi}{b} y \vec{a}_y - \frac{k_c^2}{j\beta} \sin \alpha_n x \sin \frac{n\pi}{b} y \vec{a}_z \right] e^{-j\beta z} \quad (2a)$$

$$\vec{H}_I = \sum_{n=1,2,3\dots}^N B_n \frac{\omega\epsilon}{\beta} \left[-\frac{n\pi}{b} \sin \alpha_n x \cos \frac{n\pi}{b} y \vec{a}_x + \alpha_n \cos \alpha_n x \sin \frac{n\pi}{b} y \vec{a}_y \right] e^{-j\beta z} \quad (2b)$$

$$\vec{E}_{II} = \left[\gamma \sin \gamma \left(\frac{a}{2} - x \right) \sin \frac{\pi}{d} (y - h) \vec{a}_x + \frac{\pi}{d} \cos \gamma \left(\frac{a}{2} - x \right) \cos \frac{\pi}{d} (y - h) \vec{a}_y - \frac{k_c^2}{j\beta} \cos \gamma \left(\frac{a}{2} - x \right) \sin \frac{\pi}{d} (y - h) \vec{a}_z \right] e^{-j\beta z} \quad (2c)$$

$$\vec{H}_{II} = \frac{\omega\epsilon}{\beta} \left[-\frac{\pi}{d} \cos \gamma \left(\frac{a}{2} - x \right) \cos \frac{\pi}{d} (y - h) \vec{a}_x + \gamma \sin \gamma \left(\frac{a}{2} - x \right) \sin \frac{\pi}{d} (y - h) \vec{a}_y \right] e^{-j\beta z} \quad (2d)$$

where

$$B_n = \frac{(\pi/d) 2 \cos(\gamma s/2)}{b \sin \alpha_n l \left[(\pi/d)^2 - (n\pi/b)^2 \right]} \left[\sin \frac{n\pi}{b} (h+d) + \sin \frac{n\pi}{b} h \right]$$

β , k_c and γ are related as

$$\beta^2 = k_o^2 - k_c^2 \quad , \quad k_c = 2\pi/\lambda_c$$

$$\alpha_n^2 = k_c^2 - \left(\frac{n\pi}{b} \right)^2 \quad , \quad \gamma^2 = k_c^2 - \left(\frac{\pi}{d} \right)^2$$

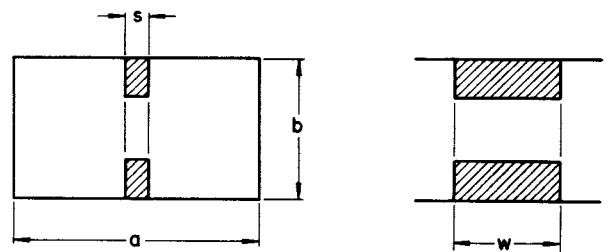


Fig. 1 Ridge waveguide E-plane discontinuity

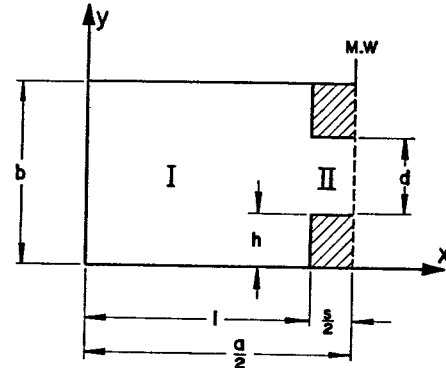


Fig. 2 Ridge waveguide with magnetic wall symmetry

Equations (1) and (2) not only give the field distribution of the dominant TE mode and dominant TM mode but also can be used to represent that of the higher order modes. The conservation of complex power technique reported in [5] can then be employed to evaluate the scattering matrix of the E-plane ridge waveguide discontinuity.

In order to check the validity of this analysis, we compare in Fig. 3 our results with those reported in [1] using the spectral domain technique. A good agreement is observed. Fig. 4 shows also a comparison between our results and experimental results for a structure with a ridge of finite metalization thickness. It is noted that there is a good agreement between the computed and the experimental results.

In contrast to the variational technique used in [7], the effect of the higher order mode coupling can be taken into account in the present analysis. This in turn allows cascaded discontinuities to be accurately analyzed. Fig. 5 shows the transmission coefficient of two E-plane discontinuities connected in cascade. It is observed that the calculated results agree well with the measured results.

III. FIELD DESCRIPTION IN UNILATERAL FINLINES

Due to the hybrid nature of the electromagnetic field in unilateral finlines, the field distribution is expressed as a summation of LSE and LSM modes. With the propagation constant calculated using the closed form expressions given in [6], and with the assumption of a constant field in the fingap and (N LSE modes + N LSM modes) in regions I, II and III of Fig. 6, the field distribution of the dominant mode can be approximated as follows:

$$\vec{E} = \vec{E}^h + \vec{E}^e, \quad \vec{H} = \vec{H}^h + \vec{H}^e$$

$$\vec{E}^h = \sum_{n=0,1,2,\dots}^N A_n \left[j \beta \varphi_n(x) \cos \frac{n\pi}{b} y \vec{a}_y + \right. \\ \left. - \frac{n\pi}{b} \varphi_n(x) \sin \frac{n\pi}{b} y \vec{a}_z \right] e^{-j\beta z} \quad (3a)$$

$$\vec{E}^e = \sum_{n=1,2,3,\dots}^N B_n \left[\frac{K_{cn}^2}{j \alpha_n} \psi_n(x) \sin \frac{n\pi}{b} y \vec{a}_x + \right. \\ \left. - \frac{n\pi}{b} \varphi_n(x) \cos \frac{n\pi}{b} y \vec{a}_y - \right. \\ \left. j \beta \varphi_n(x) \sin \frac{n\pi}{b} y \vec{a}_z \right] e^{-j\beta z} \quad (3b)$$

$$\vec{H}^h = \sum_{n=1,2,3,\dots}^N A_n \frac{\alpha_n}{\omega \mu} \left[\frac{K_{cn}^2}{j \alpha_n} \varphi_n(x) \cos \frac{n\pi}{b} y \vec{a}_x - \right. \\ \left. - \frac{n\pi}{b} \psi_n(x) \sin \frac{n\pi}{b} y \vec{a}_y - \right. \\ \left. j \beta \psi_n(x) \cos \frac{n\pi}{b} y \vec{a}_z \right] e^{-j\beta z} \quad (4a)$$

$$\vec{H}^e = \sum_{n=0,1,2,\dots}^N B_n \frac{\omega \epsilon}{\alpha_n} \left[-j \beta \psi_n(x) \sin \frac{n\pi}{b} y \vec{a}_y - \right. \\ \left. - \frac{n\pi}{b} \psi_n(x) \cos \frac{n\pi}{b} y \vec{a}_z \right] e^{-j\beta z} \quad (4b)$$

In region I

$$\varphi_n(x) = j \sin \alpha_{1n} x, \quad \psi_n(x) = \cos \alpha_{1n} x$$

$$A_n = \frac{2j\beta W_n}{[e^{+j\alpha_{1n}l_1} - e^{-j\alpha_{1n}l_1}]} \quad , \quad B_n = \frac{2(n\pi/b) W_n}{[e^{+j\alpha_{1n}l_1} - e^{-j\alpha_{1n}l_1}]} \quad (5)$$

$$W_n = \frac{\Gamma_n}{n\pi} \frac{1}{K_{cn}^2} \left[\sin \frac{n\pi}{b} (h+d) - \sin \frac{n\pi}{b} h \right]$$

In region II

$$\varphi_n(x) = [S_n e^{+j\alpha_{2n}(x-l_1)} + e^{-j\alpha_{2n}(x-l_1)}]$$

$$\psi_n(x) = [S_n e^{+j\alpha_{2n}(x-l_1)} - e^{-j\alpha_{2n}(x-l_1)}]$$

$$A_n = j \beta \frac{W_n}{(1+S_n)} \quad , \quad B_n = \frac{n\pi}{b} \frac{W_n}{(1+S_n)} \quad (6)$$

$$S_n = e^{-j2\alpha_{2n}l_2} \frac{(1-C_n) - (1+C_n) e^{-j2\alpha_{3n}l_3}}{(1+C_n) - (1-C_n) e^{-j2\alpha_{3n}l_3}} \quad (7)$$

$$C_n = \frac{\alpha_{3n}^*}{\alpha_{2n}^*} \quad \text{for LSE modes}$$

$$C_n = \epsilon_r \frac{\alpha_{2n}^*}{\alpha_{3n}^*} \quad \text{for LSM modes}$$

In region III

$$\varphi_n(x) = j \sin \alpha_{3n} (x-a), \quad \psi_n(x) = \cos \alpha_{3n} (x-a)$$

$$A_n = 2j\beta W_n Y_n \quad , \quad B_n = 2 \frac{n\pi}{b} W_n Y_n \quad (8)$$

$$Y_n = \frac{[e^{-j\alpha_{3n}l_2} + e^{j\alpha_{3n}l_2} S_n]}{[e^{-j\alpha_{3n}l_3} - e^{+j\alpha_{3n}l_3}] [1+S_n]} \quad (9)$$

where

$$\Gamma_n = 1 \text{ for } n=0 \text{ and } \Gamma_n = 2 \text{ for } n=1,2,3,\dots$$

$$K_{cn}^2 = \left(\frac{n\pi}{b} \right)^2 + \beta^2, \quad \alpha_m^2 = k_0^2 \epsilon_{ri} - K_{cn}^2$$

Having obtained the E and H field components, the characteristic impedance can be easily evaluated. In Fig. 7 we compare the characteristic impedance calculated using equation (3) and (4) with those reported in [9] using the spectral domain technique (in [9] a constant field is also assumed in the fingap). It is noted that there is a good agreement. In order to verify the validity of equations (3) and (4), we also show in Fig. 7 results calculated using the more exact analysis reported in [10]. It is concluded that equations (3) and (4) can reasonably well approximate the field in structures with small fingap ($d/b < 0.2$). This is however the case in most practical applications.

Another useful application of equations (3) and (4) is in determining the location of the plane of pure circularly polarized magnetic field, which is needed in the design of finline isolators [7].

CONCLUSIONS

Novel closed-form equations are reported for the field distribution of TM modes in ridge waveguides as well as the dominant mode in unilateral finlines. Numerical results are presented which confirm the usefulness of these equations in the calculation of the characteristic impedance in unilateral finlines and in the analysis of E-plane ridge waveguide discontinuities.

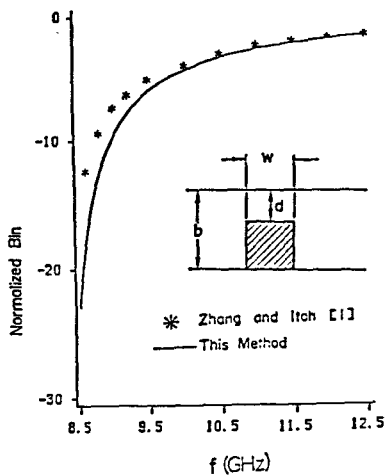


Fig. 3 Normalized susceptance of an E-plane ridge waveguide discontinuity: $a=22.86\text{mm}$, $b=10.16\text{mm}$, $h=0.0$, $S=0.0$, $l=11.43\text{mm}$, $d=2.79\text{mm}$, $w=1.7\text{mm}$.

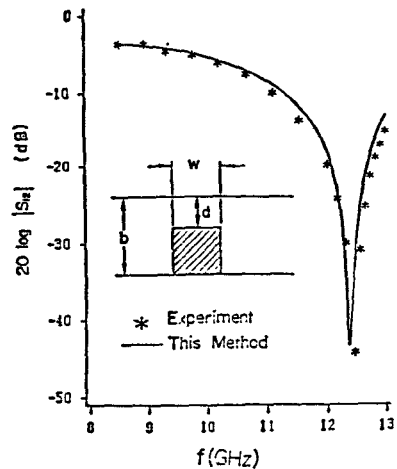


Fig. 4 Magnitude of transmission coefficient of an E-plane ridge waveguide discontinuity: $a=22.86\text{mm}$, $b=10.16\text{mm}$, $h=0.0$, $S=1.0287\text{mm}$, $l=10.40\text{mm}$, $d=4.14\text{mm}$, $w=1.27\text{mm}$.

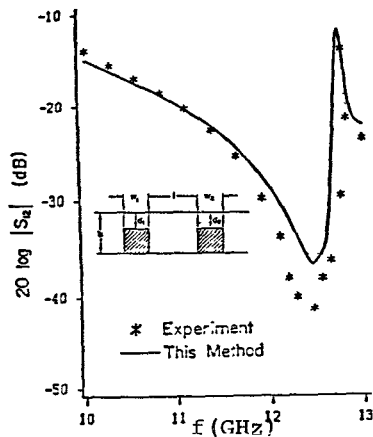


Fig. 5 Magnitude of transmission coefficient of a cascaded E-plane ridge waveguide discontinuity: $a=22.86\text{mm}$, $b=10.16\text{mm}$, $h=0.0$, $S=1.0287\text{mm}$, $l=10.40\text{mm}$, $d=4.14\text{mm}$, $w=1.27\text{mm}$, $d_1=d_2=4.14\text{mm}$, $l'=12.192\text{mm}$, $w_1=w_2=1.524$.

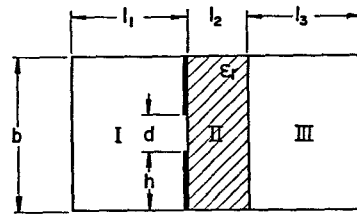


Fig. 6 A unilateral finline structure

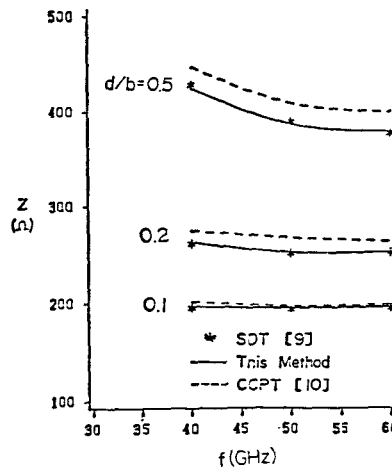


Fig. 7 Characteristic impedance versus frequency in unilateral finlines: $a=2b=4.7752\text{mm}$, $l_2=0.127\text{mm}$, $l_1=2.3876\text{mm}$, $\epsilon_r=2.2$

ACKNOWLEDGEMENT

The authors would like to thank the management of COM DEV Ltd. for permission to present this paper.

REFERENCES

- [1] Q. Zhang and T. Itoh, *IEEE Trans.*, vol. MTT-35, pp.138-150, February 1987.
- [2] J. Bornemann and F. Arndt, *IEEE Trans.*, vol. MTT-35, pp.561-567, June 1987.
- [3] W. J. Getsinger, *IRE Trans.*, vol. MTT-10, pp.41-50, January 1962.
- [4] Y. Konishi and H. Matsumura, *IEEE Trans.*, vol. MTT-27, pp.168-170, February 1979.
- [5] R. R. Mansour and R. H. MacPhie, *IEEE Trans.*, vol. MTT-34, pp.1490-1498, December 1986.
- [6] P. Pramanick and P. Bahartia, *IEEE Trans.*, vol. MTT-33, pp.24-30, January 1985.
- [7] A. Beyer and I. Wolf, European Microwave Conference Proc., pp.321-326, 1981.
- [8] K. Chang and P. J. Khan, *IEEE Trans.*, vol. MTT-22, pp.536-541, May 1974.
- [9] J. B. Knorr and P. M. Shayda, *IEEE Trans.*, vol. MTT-28, pp.737-743, July 1980.
- [10] R. R. Mansour and R. H. MacPhie, *IEEE Trans.*, vol. MTT-34, pp. 1382-1391, December 1987.